PHYSICAL REVIEW D **86,** 085029 (2012)

# Dynamics of the chiral magnetic effect in a weak magnetic field

Harmen J. Warringa*

*Frankfurt Institute for Advanced Studies (FIAS), Frankfurt am Main, Germany*
*and Institut für Theoretische Physik, Goethe-Universität, Frankfurt am Main, Germany*

(Received 5 June 2012; published 15 October 2012)

We investigate the real-time dynamics of the chiral magnetic effect in quantum electrodynamics and quantum chromodynamics. We consider a field configuration of parallel (chromo)electric and (chromo) magnetic fields with a weak perpendicular electromagnetic magnetic field. The chiral magnetic effect induces an electromagnetic current along this perpendicular magnetic field, which we will compute using linear response theory. We discuss specific results for a homogeneous sudden switch-on and a pulsed (chromo)electric field in a static and homogeneous (chromo)magnetic field. Our methodology can be easily extended to more general situations. The results are useful for investigating the chiral magnetic effect with heavy ion collisions and with lasers that create strong electromagnetic fields. As a side result we obtain the rate of chirality production for massive fermions in parallel electric and magnetic fields that are static and homogeneous.

DOI: 10.1103/PhysRevD.86.085029 PACS numbers: 12.20.Ds, 11.15.Tk, 12.38.Lg

## I. INTRODUCTION

In quantum electrodynamics (QED) and quantum chromodynamics (QCD) certain gauge field configurations will induce chirality as follows from the axial Ward identity [1,2]. These gauge field configurations have a net topological charge density, which means that the contraction of the field strength tensor with its dual is nonvanishing. An example of such a gauge field configuration is one in which the (chromo)electric and (chromo)magnetic fields are parallel. For massless particles, chirality is the asymmetry between the number of particles plus antiparticles with right-handed helicity and the number of particles plus antiparticles with left-handed helicity. Here right-handed helicity means that spin and momentum are parallel, whereas left-handed helicity means they are antiparallel. If a system of charged fermions possesses a net chirality, then an applied (electromagnetic) magnetic field will induce an electromagnetic current in the direction of the magnetic field [3]. This is called the chiral magnetic effect. In magnetic fields that are large enough to fully polarize the fermions, one can easily convince oneself that the magnitude of this current is equal to the chirality times the absolute value of the fermion charge [4].

To improve the understanding of the chiral magnetic effect it is important to obtain the magnitude of the induced electromagnetic current in different situations. In many studies of the chiral magnetic effect the chirality is introduced by hand through a chiral chemical potential $\mu_5$ [3,5,6]. However, in order to get a full understanding of the chiral magnetic effect, one should include the dynamics that leads to a net chirality. Such dynamical studies have been performed in Euclidean space-time using lattice QCD [7] and with analytic methods, both in Euclidean [8,9] and Minkowski [10] space-time.

In this article we will study the real-time dynamics of the chiral magnetic effect with an analytic method. We will consider a specific gauge field configuration of parallel homogeneous (chromo)electric and (chromo)magnetic fields that are pointing in the z direction. These parallel fields are the source of the chirality. The (chromo)magnetic field is assumed to be constant in time, but the (chromo)electric field can have any time dependence. Perpendicular to these fields we will consider an electromagnetic magnetic field with arbitrary time dependence that points in the y direction. We have sketched the situation in Fig. 1. The goal of this article is to obtain the current density in the y direction, which is due to the chiral magnetic effect.

The chiral magnetic effect will take place unsuppressed if the fields have a magnitude that is at least of order of the fermion mass squared. In the near future, one hopes to create such enormous electromagnetic fields with high intensity lasers (see e.g., Ref. [11]). If one could engineer a field configuration like the one of Fig. 1 with these lasers, one could falsify the chiral magnetic effect in QED in a controlled environment. In heavy ion collisions a similar configuration built out of flux tubes of parallel chromoelectric and chromomagnetic fields is induced [12]. Perpendicular to these color fields a large electromagnetic magnetic field is generated through the currents created by the colliding charged ions [4,13].

In QCD the probability of generating gauge field configurations with positive and negative topological charge is equal (assuming $\theta = 0$). Hence in heavy ion collisions, the current along the perpendicular field vanishes on average. However, because of fluctuations in the initial state [12] and the presence of sphalerons [14], the topological charge fluctuates. Hence the current along the perpendicular magnetic field will fluctuate as well. That will lead to

*warringa@th.physik.uni-frankfurt.de

 

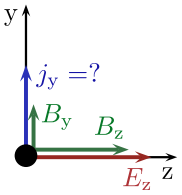


FIG. 1 (color online). Field configuration in which the chiral magnetic effect is studied in this article. The electric field along the z-direction ($E_z$) is homogeneous and can have arbitrary time dependence. The magnetic field along the z-direction is static and homogeneous. The goal is to compute the current density $j_y$ along the magnetic field in the y-direction ($B_y$).

differences in net electric charge between the two sides of the reaction plane (the plane in which the beam axis and the impact parameter lie) on an event-by-event basis [15]. This effect can be analyzed experimentally through a charge correlation study [16]. Charge correlations have indeed been observed at both the Relativistic Heavy Ion Collider [17] and the Large Hadron Collider [18]. However, currently it is not clear if these correlations are caused by the chiral magnetic effect or by another mechanism [19]. A possible observation of the chiral magnetic effect in QCD can teach us about the relevance of configurations with topological charge.

Theoretically, the field configuration displayed in Fig. 1 is interesting, because when all fields are static and homogeneous it is possible to obtain a full analytic expression for the induced current density along the perpendicular magnetic field [10]. The current density behaves exactly according to the qualitative expectations of the chiral magnetic effect. For example, for a large perpendicular magnetic field the magnitude of the current was found to be equal to the chirality times the absolute value of the charge of the fermion. Furthermore, the current density is suppressed by the fermion mass, and vanishes if there is no chirality production.

The calculation in Ref. [10] was built upon a nice argument based on Lorentz transformations and the particle production rate in parallel, homogeneous and static fields. However, this argument cannot be applied to more general situations that are useful to investigate. For example, in heavy ion collisions the magnetic field has a strong time dependence. Furthermore, with high-intensity lasers one will create inhomogeneous and time-dependent fields. And for purely academic reasons it is of interest to analyze the real-time dynamics of the chiral magnetic effect in a spherical symmetric background gluon field that carries one unit of topological charge, and is a solution of the Yang-Mills equations.

To obtain the induced current density along the magnetic field in a general situation one can in principle just solve the Dirac equation numerically, and construct the current from the solutions. However, this might be quite difficult in practice. In order to make progress, we will start a program to investigate the chiral magnetic effect using linear response theory. We will expand to first order in the electromagnetic field that is the source of the perpendicular magnetic field. In this way we can investigate the chiral magnetic effect for weak perpendicular magnetic fields that have arbitrary space and time dependence. In practical terms we will confirm in this article the results of Ref. [10] in the weak magnetic field limit. Furthermore we will analyze the chiral magnetic effect in pulsed electric fields.

Most of the calculations in this article will be performed in QED. From the QED results it is easy to obtain the results for QCD as in Ref. [10] and as explained at the end of the introduction. We hope that our results will inspire the reader to perform other studies of the chiral magnetic effect using linear response theory.

This article is organized as follows. In Sec. II, we will construct the fermion propagator of QED in a background of parallel electric and magnetic fields. To support *Ansätze* made in Ref. [10], we compute the electromagnetic current density for massive fermions analytically in Sec. III. In this section we will also obtain an analytic expression for the rate of chirality production for massive fermions in parallel electric and magnetic fields. In Sec. IV, we will then apply linear response theory to obtain the induced current density along a magnetic field that is perpendicular to these background fields. We will discuss our numerical results in Sec. V and show among other things that we can reproduce the results of Ref. [10] in the limit of weak magnetic fields. The conclusions of this work can be found in Sec. VI.

Some details of this work can be found in the appendices. In Appendix A, we give several relations involving the wave functions in a magnetic field. Finally in Appendix B, we discuss the wave functions in a sudden switch-on electric field.

The notational conventions we will use in this article are summarized below. We also explain the relation between the QED and the QCD setup below.

### A. Notation

We will use as a metric $g^{\mu\nu} = \mathrm{diag}(1, -1, -1, -1)$. We write $p = p^\mu = (p^0, \boldsymbol{p})$ to denote a four-vector. A component of a four-vector will be written with either numbers or with an italic sub- or superscript. For example, $p^z = p^3 = -p_z = -p_3$. We will use roman subscripts to indicate a component of a three-vector, i.e., $\boldsymbol{p} = (p_\mathrm{x}, p_\mathrm{y}, p_\mathrm{z}) = (p^\mathrm{x}, p^\mathrm{y}, p^\mathrm{z})$. Hence $p^\mathrm{z} = p_\mathrm{z} = -p_z$. Likewise we write $\boldsymbol{x} = (x_\mathrm{x}, x_\mathrm{y}, x_\mathrm{z})$ which we most often simplify to $\boldsymbol{x} = (\mathrm{x}, \mathrm{y}, \mathrm{z})$.

### B. Relation between QCD and QED setup

As in Ref. [10] we consider an Abelianized gluon field configuration of the form $A^a_\mu = \mathcal{A}_\mu n^a$ in the QCD setup. Here $n^a$ denotes a direction in the adjoint space. Since the electromagnetic current density, the object we wish to compute, is gauge invariant, we can perform a gauge

transformation to rotate $n^a$ to the $a = 3$ direction. From the covariant derivative $D_\mu = \partial_\mu - ig\mathcal{A}_\mu t^3$, it then follows that the red quarks effectively experience an electromagnetic field of magnitude $qA_\mu = -g\mathcal{A}_\mu/2$ whereas the green quarks experience an effective electromagnetic field with size $qA_\mu = g\mathcal{A}_\mu/2$. The blue quarks are not affected by the field. Here $q$ is the charge of the fermion and $g$ is the QCD coupling constant. The current density along the perpendicular magnetic field in the QCD setup can thus be obtained from the QED result, yielding

$$j_{\mathrm{y,QCD}} = 2\sum_f j_{\mathrm{y,QED}}(qE_{\mathrm{z}} = g\mathcal{E}_{\mathrm{z}}/2, \quad qB_{\mathrm{z}} = g\mathcal{B}_{\mathrm{z}}/2, q = q_f, m = m_f). \tag{1}$$

Here $f$ is a sum over quark flavors, $m$ is the mass, and $(\mathcal{E}_{\mathrm{z}})E_{\mathrm{z}}$ and $(\mathcal{B}_{\mathrm{z}})B_{\mathrm{z}}$ denote respectively the z component of the (chromo)electric and (chromo)magnetic field.

There is an important difference between the QED and QCD setup. In QED the electromagnetic current has also a component in the z direction due to acceleration of charges along the electric field. In the QCD setup however, this contribution to the electromagnetic current vanishes due to a cancellation from the contribution of red and green quarks. The electromagnetic current in the QCD setup has thus only a component in the y direction due to the chiral magnetic effect.

## II. FERMION PROPAGATOR IN ELECTROMAGNETIC BACKGROUND

The goal of this section is to obtain a convenient expression for the fermion propagator in a background of electric and magnetic fields both pointing in the z direction. We will consider a homogeneous static magnetic field, $\boldsymbol{B} = B_{\mathrm{z}}\mathbf{e}_{\mathrm{z}}$. The electric field is assumed to be homogeneous as well with an arbitrary time dependence, $\boldsymbol{E} = E(t)\mathbf{e}_{\mathrm{z}}$. The corresponding gauge fields will be chosen as follows: $A^0 = 0$ and $\boldsymbol{A} = (0, B_{\mathrm{z}}x, A_{\mathrm{z}}(t))$ with $\lim_{t\to-\infty}A_{\mathrm{z}}(t) = 0$ so that $E(t) = -\partial_t A_{\mathrm{z}}(t)$.

In this section we will first compute the Dirac spinors in this electromagnetic background. Using these spinors we will construct the quantum field for fermions, from which we will derive the different fermion propagators.

### A. Dirac spinors

The spinors $\psi(x)$ can be obtained from the Dirac equation which reads

$$(\mathrm{i}\gamma^\mu D_\mu - m)\psi(x) = 0, \tag{2}$$

where the covariant derivative $D_\mu = \partial_\mu + \mathrm{i}qA_\mu$ with $q$ the electric charge of the fermion.

To solve the Dirac equation in the background given above we will apply the Ritus method [20]. This method amounts to making the following *Ansatz* for the particle spinors (+) with momentum $\boldsymbol{p}$ and antiparticle spinors (−) with momentum $-\boldsymbol{p}$:

$$\psi^+_{ps}(x) = F^+_{\boldsymbol{p}}(t)G_{\boldsymbol{p}}(\mathrm{x})\mathrm{e}^{\mathrm{i}p_{\mathrm{y}}\mathrm{y}+\mathrm{i}p_{\mathrm{z}}\mathrm{z}}u_s(\tilde{p}_+), \tag{3}$$

$$\psi^-_{ps}(x) = F^-_{\boldsymbol{p}}(t)G_{\boldsymbol{p}}(\mathrm{x})\mathrm{e}^{\mathrm{i}p_{\mathrm{y}}\mathrm{y}+\mathrm{i}p_{\mathrm{z}}\mathrm{z}}v_s(\tilde{p}_-). \tag{4}$$

Here the four-vector $\tilde{p}^\mu_\pm = (\kappa, 0, \mp\lambda, 0)$, and $u_s(\tilde{p}_+)$ and $v_s(\tilde{p}_-)$ denote the usual particle and antiparticle spinors of the free Dirac equation with momentum $\tilde{p}_\pm$. The free Dirac spinors satisfy the following equations:

$$(\tilde{\not{p}}_+ - m)u_s(\tilde{p}_+) = 0, \quad (\tilde{\not{p}}_- + m)v_s(\tilde{p}_-) = 0. \tag{5}$$

Furthermore, $\kappa$ and $\lambda$ are constants that depend on $\boldsymbol{p}$, and will be determined below. Finally, $F^\pm_{\boldsymbol{p}}(t)$ is a $4\times4$ matrix that has to commute with $\gamma^1$ and $\gamma^2$, and $G_{\boldsymbol{p}}(\mathrm{x})$ a $4\times4$ matrix that should commute with $\gamma^0$ and $\gamma^3$.

By inserting the Ritus *Ansatz* into the Dirac equation it follows that this *Ansatz* is indeed a general solution if the matrices $F^\pm_{\boldsymbol{p}}(t)$ and $G_{\boldsymbol{p}}(\mathrm{x})$ obey the following two equations

$$[\mathrm{i}\gamma^0\partial_t - \gamma^3(p_{\mathrm{z}} - qA_{\mathrm{z}}(t))]F^\pm_{\boldsymbol{p}}(t) = \pm\kappa F^\pm_{\boldsymbol{p}}(t)\gamma^0, \tag{6}$$

$$[\mathrm{i}\gamma^1\partial_{\mathrm{x}} - \gamma^2(p_{\mathrm{y}} - qB_{\mathrm{z}}\mathrm{x})]G_{\boldsymbol{p}}(\mathrm{x}) = \lambda G_{\boldsymbol{p}}(\mathrm{x})\gamma^2. \tag{7}$$

We will solve these two equations explicitly below.

By multiplying Eq. (5) from the left with $(\tilde{\not{p}}_\pm \pm m)$ it follows that $\tilde{p}^2_\pm = m^2$, so that $\kappa^2 = \lambda^2 + m^2$. We will normalize the free Dirac spinors as in Ref. [21]. In that convention the polarization sums, which are the only nontrivial property of the free spinors required in this article, read

$$\sum_{s=\pm} u_s(p)\bar{u}_s(p) = (\not{p} + m), \tag{8}$$

$$\sum_{s=\pm} v_s(p)\bar{v}_s(p) = (\not{p} - m). \tag{9}$$

In the remaining part of this subsection, we will determine the matrices $F^\pm_{\boldsymbol{p}}(t)$ and $G_{\boldsymbol{p}}(\mathrm{x})$, and the values of $\kappa$ and $\lambda$ explicitly. Without loss of generality both $F^\pm_{\boldsymbol{p}}(t)$ and $G_{\boldsymbol{p}}(\mathrm{x})$ can be taken diagonal.

#### 1. Computation of $G_{\boldsymbol{p}}(\mathrm{x})$

From Eq. (7) it follows that $G_{\boldsymbol{p}}(\mathrm{x})$ is a function of $\mathrm{x} - p_{\mathrm{y}}/qB_{\mathrm{z}}$. Therefore let us write the diagonal elements of $G_{\boldsymbol{p}}(\mathrm{x})$ as $g_a(\mathrm{x} - p_{\mathrm{y}}/qB_{\mathrm{z}})$ with $a = 1\ldots4$. By multiplying Eq. (7) from the left with $\gamma^2$ one finds that

$$(\partial_{\mathrm{x}} + qB_{\mathrm{z}}\mathrm{x})g_1(\mathrm{x}) = \lambda g_4(\mathrm{x}), \tag{10}$$

$$(\partial_{\mathrm{x}} - qB_{\mathrm{z}}\mathrm{x})g_4(\mathrm{x}) = -\lambda g_1(\mathrm{x}). \tag{11}$$

Since the other two components satisfy the same set of equations, $g_2(\mathrm{x})$ is proportional to $g_4(\mathrm{x})$ and $g_3(\mathrm{x})$ is

proportional to $g_1(\mathrm{x})$. In order to ensure that $G_{\boldsymbol{p}}(\mathrm{x})$ commutes with $\gamma^0$ and $\gamma^3$ as required, we have to take $g_2(\mathrm{x}) = g_4(\mathrm{x})$ and $g_1(\mathrm{x}) = g_3(\mathrm{x})$.

By combining Eqs. (10) and (11) one finds that $g_a(\mathrm{x})$ satisfies the following equation:

$$(-\partial_{\mathrm{x}}^2 + q^2 B_{\mathrm{z}}^2 \mathrm{x}^2 - sqB_{\mathrm{z}}) g_a(\mathrm{x}) = \lambda^2 g_a(\mathrm{x}), \tag{12}$$

with $s = 1$ for $a = 1, 3$ and $s = -1$ for $a = 2, 4$. Equation (12) is the eigenvalue equation of a harmonic oscillator with angular frequency $|qB_{\mathrm{z}}|$. The eigenvalues are given by $\lambda^2 = (2n+1)|qB_{\mathrm{z}}| - sqB_{\mathrm{z}}$ with quantum number $n = 0, 1, 2, \ldots$ The corresponding eigenfunctions $\phi_n(\mathrm{x})$ read

$$\phi_n(\mathrm{x}) = \frac{1}{\sqrt{2^n n!}} \left(\frac{|qB_{\mathrm{z}}|}{\pi}\right)^{1/4} H_n\left(\sqrt{|qB_{\mathrm{z}}|}\mathrm{x}\right) \times \exp\left(-\frac{1}{2}|qB_{\mathrm{z}}|\mathrm{x}^2\right), \tag{13}$$

where $H_n(z)$ denotes a Hermite polynomial of degree $n$. For convenience we define $\phi_{-1}(\mathrm{x}) = 0$. The eigenfunctions $\phi_n(\mathrm{x})$ are normalized as

$$\int_{-\infty}^{\infty} \mathrm{d}\mathrm{x} \phi_n(\mathrm{x}) \phi_m(\mathrm{x}) = \delta_{nm}, \tag{14}$$

and satisfy the completeness relation

$$\sum_{n=0}^{\infty} \phi_n(\mathrm{x}) \phi_n(\mathrm{x}') = \delta(\mathrm{x} - \mathrm{x}'). \tag{15}$$

Let us now write $\lambda^2 = 2k|qB_{\mathrm{z}}|$ with $k = 0, 1, 2, \ldots$ The full solution to Eq. (12) can be found by using that $g_1(\mathrm{x})$ and $g_4(\mathrm{x})$ must have the same value of $\lambda^2$. This gives for $qB_{\mathrm{z}} > 0$, $g_1(\mathrm{x}) = c_1 \phi_k(\mathrm{x})$ and $g_4(\mathrm{x}) = c_4 \phi_{k-1}(\mathrm{x})$. Choosing the normalization such that $c_1 = 1$, it follows from Eq. (10) that $c_4 = c_1 = 1$. In this way one obtains also the sign of $\lambda$, giving $\lambda = \mathrm{sgn}(qB_{\mathrm{z}})\sqrt{2|qB_{\mathrm{z}}|k}$. As long as $qB_{\mathrm{z}} > 0$ one then finds $g_a(\mathrm{x}) = \phi_k(\mathrm{x})$ for $a = 1, 3$ and $g_a(\mathrm{x}) = \phi_{k-1}(\mathrm{x})$ for $a = 2, 4$. If $qB_{\mathrm{z}} < 0$ the solution is $g_a(\mathrm{x}) = \phi_{k-1}(\mathrm{x})$ for $a = 1, 3$ and $g_a(\mathrm{x}) = \phi_k(\mathrm{x})$ for $a = 2, 4$.

The diagonal matrix $G(\mathrm{x})$ can now be written in the following compact notation:

$$G_{\boldsymbol{p}}(\mathrm{x}) = \sum_{s=\pm} g_{\boldsymbol{p}s}(\mathrm{x}) \mathcal{P}_g^s, \tag{16}$$

where we introduced $g_{\boldsymbol{p}+}(\mathrm{x}) = \phi_k(\mathrm{x} - \frac{p_y}{qB_{\mathrm{z}}})$ and $g_{\boldsymbol{p}-}(\mathrm{x}) = \phi_{k-1}(\mathrm{x} - \frac{p_y}{qB_{\mathrm{z}}})$. The projection operators $\mathcal{P}_g^s$ are given by $\mathcal{P}_g^s = (1 + \mathrm{i}s\,\mathrm{sgn}(qB_{\mathrm{z}})\gamma^1\gamma^2)/2$.

### 2. Computation of $F_{\boldsymbol{p}}^{\pm}(t)$

Let us write the diagonal elements of the matrix $F_{\boldsymbol{p}}^{\pm}(t)$ as $f_a^{\pm}(t)$ with $a = 1 \ldots 4$. Multiplying Eq. (6) from the left with $\gamma^0$ yields

$$[\mathrm{i}\partial_t + p_{\mathrm{z}} - qA_{\mathrm{z}}(t)] f_1^{\pm}(t) = \pm\kappa f_3^{\pm}(t), \tag{17}$$

$$[\mathrm{i}\partial_t - p_{\mathrm{z}} + qA_{\mathrm{z}}(t)] f_3^{\pm}(t) = \pm\kappa f_1^{\pm}(t). \tag{18}$$

Since the other two components satisfy the same set of equations it follows that $f_2^{\pm}(t) \propto f_3^{\pm}(t)$ and $f_4^{\pm}(t) \propto f_1^{\pm}(t)$. In order to ensure that $F_{\boldsymbol{p}}^{\pm}(t)$ commutes with $\gamma^1$ and $\gamma^2$ we have to take $f_2^{\pm}(t) = f_3^{\pm}(t)$ and $f_4^{\pm}(t) = f_1^{\pm}(t)$. We can therefore write

$$F_{\boldsymbol{p}}^{\pm}(t) = \sum_{s=\pm} f_{\boldsymbol{p}s}^{\pm}(t) \mathcal{P}_f^s, \tag{19}$$

where $f_{\boldsymbol{p}+}^{\pm}(t) = f_1^{\pm}(t)$, $f_{\boldsymbol{p}-}^{\pm}(t) = f_3^{\pm}(t)$ and the projection operators $\mathcal{P}_f^s = (1 + s\gamma^3\gamma^0)/2$.

By taking the complex conjugate of Eqs. (17) and (18) it can be seen that $f_{\boldsymbol{p}s}^{-}(t)$ satisfies the same two differential equations as $f_{\boldsymbol{p}-s}^{+}(t)^*$. Hence both functions are proportional to each other. Since it is natural to normalize the particle and antiparticle spinors in the same way, we take

$$f_{\boldsymbol{p}s}^{-}(t) = f_{\boldsymbol{p}-s}^{+}(t)^*. \tag{20}$$

We will use this relation throughout to express our final results in terms of particle wave functions only.

From Eqs. (17) and (18) it also follows that the sum $|f_{\boldsymbol{p}+}^{\pm}(t)|^2 + |f_{\boldsymbol{p}-}^{\pm}(t)|^2$ is independent of time. As it turns out it will be convenient to normalize this combination as

$$|f_{\boldsymbol{p}+}^{\pm}(t)|^2 + |f_{\boldsymbol{p}-}^{\pm}(t)|^2 = 2. \tag{21}$$

In the next subsection we will check that the normalizations we have made are consistent, by verifying that the quantum fields satisfy the canonical anticommutation relations.

In general the wave functions $f_{\boldsymbol{p}s}^{\pm}(t)$ can only be obtained numerically. There are only a few cases in which analytic solutions are known. We will now discuss a few of them.

For vanishing electromagnetic field, $A_{\mathrm{z}}(t) = 0$, combining Eqs. (17) and (18) gives

$$[-\partial_t^2 - p_{\mathrm{z}}^2] f_{\boldsymbol{p}s}^{\pm}(t) = \kappa^2 f_{\boldsymbol{p}s}^{\pm}(t), \tag{22}$$

with $s = \pm$. The solution of the last equation is a linear combination of phase factors $\exp(\pm\mathrm{i}p_0 t)$, where $p_0 = \sqrt{\kappa^2 + p_{\mathrm{z}}^2}$. The two different solutions correspond to particles and antiparticles; hence $f_s^{\pm}(t) = c_s^{\pm} \exp(\mp\mathrm{i}p_0 t)$ where $c_s^{\pm}$ is a normalization constant. From Eq. (17) it follows that the ratio of the normalization constants is $c_+^{\pm}/c_-^{\pm} = \kappa/(p_0 \pm p_{\mathrm{z}})$. Applying Eq. (21) gives $(c_+^{\pm})^2 + (c_-^{\pm})^2 = 2$, so that

$$f_{\boldsymbol{p}s}^{\pm}(t) = \sqrt{\frac{p_0 \mp sp_{\mathrm{z}}}{p_0}} \exp(\mp\mathrm{i}p_0 t). \tag{23}$$

If $\kappa = 0$, the two differential equations for $f_{\boldsymbol{p}s}^{\pm}(t)$ decouple. In that case Eqs. (17) and (18) can be integrated straightforwardly, yielding

$$f^{\pm}_{ps}(t)|_{\kappa=0} = \sqrt{2}\exp\left[\mp i|p_z|t - is\int_{-\infty}^{t} dt' qA_z(t')\right]\theta(\mp s p_z). \tag{24}$$

In a sudden switch-on electric field the wave functions $f^{\pm}_{ps}(t)$ are known analytically [22]. We review the calculation in Appendix B. It is also possible to obtain an analytic solution in a pulsed field of the form $E_z(t) = E_z/\cosh^2(t/\tau)$ [23].

### B. Quantum field

The Dirac field in the electromagnetic background is given by

$$\Psi(x) = \sum_{s=\pm}\sum_{p}\frac{1}{\sqrt{2\kappa_p}}\left[b_{ps}\psi^{+}_{ps}(x) + d^{\dagger}_{-ps}\psi^{-}_{ps}(x)\right], \tag{25}$$

where we introduced $\sum_p \equiv \sum_{k=0}^{\infty}\int\frac{dp_y}{2\pi}\int\frac{dp_z}{2\pi}$ and $\kappa_p = \kappa$. Here $\psi^{\pm}_{ps}(x)$ are the particle $(+)$ and antiparticle $(-)$ spinors in the background field, which are given explicitly in Eqs. (3) and (4). The operators $b_{ps}$ and $d_{ps}$ denote respectively the annihilation operators for particles and antiparticles with momentum $\boldsymbol{p}$ and spin $s$ in a background magnetic field. The creation operator for antiparticles in Eq. (25) has negative momentum, reflecting the fact that in our notation $\psi^{-}_{ps}(x)$ denotes an antiparticle spinor with momentum $-\boldsymbol{p}$.

The creation and annihilation operators satisfy the following anticommutation relations:

$$\{b_{ps}, b^{\dagger}_{p's'}\} = \{d_{ps}, d^{\dagger}_{p's'}\} = (2\pi)^2\delta_{kk'}\delta(p_y - p'_y)\delta(p_z - p'_z)\delta_{ss'}. \tag{26}$$

All other anticommutation relations vanish.

To check that all normalization conditions are consistent we will verify that the quantum field given in Eq. (25) satisfies the canonical equal-time anticommutation relation, which reads

$$\{\Psi_a(t,\boldsymbol{x}), \Psi^{\dagger}_b(t,\boldsymbol{x}')\} = \delta_{ab}\delta^3(\boldsymbol{x}-\boldsymbol{x}'). \tag{27}$$

Inserting the explicit expression of the quantum field and using the properties of the creation and annihilation operators gives

$$\{\Psi(t,\boldsymbol{x}), \Psi^{\dagger}(t,\boldsymbol{x}')\} = \sum_{u,s=\pm}\sum_{p}\frac{1}{2\kappa_p}\psi^{u}_{ps}(t,\boldsymbol{x})\psi^{u}_{ps}(t,\boldsymbol{x}')^{\dagger}. \tag{28}$$

Inserting the explicit solution for the spinors, and summing over spins by applying Eqs. (8) and (9) yields

$$\{\Psi(t,\boldsymbol{x}), \Psi^{\dagger}(t,\boldsymbol{x}')\} = \sum_{u=\pm}\sum_{p}\frac{1}{2\kappa_{\mathbf{p}}}e^{ip_y(y-y')+ip_z(z-z')} \times\{uF^{u}_{p}(t)\gamma^0 F^{u}_{p}(t)^{\dagger}[mG_p(x)G_p(x') - \lambda G_p(x)\gamma^2 G_p(x')] + \kappa_p F^{u}_{p}(t)F^{u}_{p}(t)^{\dagger}G_p(x)G_p(x')\}. \tag{29}$$

The last equation can be simplified by inserting the explicit expression for $F^{\pm}_{p}(t)$. In this way we find that

$$\frac{1}{2}\sum_{u=\pm}F^{u}_{p}(t)F^{u}_{p}(t)^{\dagger} = \mathbb{1}_4, \tag{30}$$

$$\sum_{u=\pm}uF^{u}_{p}(t)\gamma^0 F^{u}_{p}(t)^{\dagger} = 0. \tag{31}$$

To obtain the last two equations, we have used that by combining Eqs. (20) and (21) it can be shown that

$$|f^{+}_{ps}(t)|^2 + |f^{-}_{ps}(t)|^2 = 2, \tag{32}$$

$$f^{+}_{ps}(t)f^{+}_{p-s}(t)^{*} = f^{-}_{ps}(t)f^{-}_{p-s}(t)^{*}. \tag{33}$$

Inserting Eqs. (30) and (31) into Eq. (29) yields

$$\{\Psi(t,\boldsymbol{x}), \Psi^{\dagger}(t,\boldsymbol{x}')\} = \sum_{p}e^{ip_y(y-y')+ip_z(z-z')}G_p(x)G_p(x'). \tag{34}$$

By using the explicit expression for $G_p(x)$ and applying the completeness relation Eq. (15), the canonical anticommutation relation, Eq. (27), follows directly. Hence the normalizations we have chosen are consistent.

### C. Propagator

Let us introduce the following definitions for the two-point correlation functions:

$$S^{+}_{ab}(x,x') \equiv \langle 0|\Psi_a(x)\bar{\Psi}_b(x')|0\rangle, \tag{35}$$

$$S^{-}_{ab}(x,x') \equiv \langle 0|\bar{\Psi}_b(x')\Psi_a(x)|0\rangle. \tag{36}$$

Here $|0\rangle$ denotes the in-vacuum, which in this article is the vacuum before the electric field has been switched on. The different propagators (retarded, advanced, Feynman) can be found by the appropriate linear combinations of the two-point functions. By applying Eq. (25) it follows that the two-point correlation functions expressed in terms of Dirac spinors read

$$S^{\pm}_{ab}(x,x') = \sum_{s=\pm}\sum_{p}\frac{1}{2\kappa_p}[\psi^{\pm}_{ps}(x)]_a[\psi^{\pm}_{ps}(x')^{\dagger}\gamma^0]_b. \tag{37}$$

By inserting the explicit expressions for the Dirac spinors, and summing over spins, the two-point correlation functions become

$$S^{\pm}(x,x') = \sum_{p} \frac{1}{2\kappa_p} e^{ip_y(y-y')+ip_z(z-z')} F^{\pm}_{p}(t) G_{p}(x) \times (\tilde{\not{p}}_{\pm} \pm m)\gamma^0 F^{\pm}_{p}(t')^{\dagger}\gamma^0 G_{p}(x'). \quad (38)$$

To evaluate the current density and related quantities, one has to contract a two-point correlation function with an arbitrary combination of gamma matrices denoted by $\Gamma$. These quantities can be expressed in terms of $S^{\pm}(x,x')$ in the following charge symmetric way:

$$\langle 0|\bar{\Psi}(t,\boldsymbol{x}')\Gamma\Psi(t,\boldsymbol{x})|0\rangle = -\frac{1}{2}\sum_{u=\pm} u\,\mathrm{tr}[S^{u}(t,\boldsymbol{x};t,\boldsymbol{x}')\Gamma] + \frac{1}{2}\mathrm{tr}[\gamma^0\Gamma]\delta(\boldsymbol{x}-\boldsymbol{x}'). \quad (39)$$

For the current density $j^{\mu}$ we have $\Gamma = q\gamma^{\mu}$, for the chirality $n_5$ we have $\Gamma = \gamma^0\gamma^5$, and for the pseudoscalar condensate $\Gamma = i\gamma^5$. Only for $\Gamma = \gamma^0$ the second trace in Eq. (39) does not vanish.

## III. CURRENT AND AXIAL ANOMALY IN PARALLEL ELECTRIC AND MAGNETIC FIELD

We will now compute the induced current density, chirality density and pseudoscalar condensate in the background of parallel homogeneous time-dependent electric and static magnetic fields. To compute these quantities we need to evaluate the trace of $S^{\pm}(x,x')\Gamma$ as follows from Eq. (39). This trace can be easily performed using a symbolic manipulation program such as Mathematica. Inserting the explicit forms of $F^{\pm}_{p}(t)$ and $G_{p}(x)$ gives

$$\mathrm{tr}[S^{\pm}(x,x')\gamma^3] = -\frac{1}{2}\sum_{p}\sum_{r,s=\pm} e^{ip_y(y-y')+ip_z(z-z')} \times s f^{\pm}_{ps}(t) f^{\pm}_{ps}(t')^{*} g_{pr}(x) g_{pr}(x'), \quad (40)$$

$$\mathrm{tr}[S^{\pm}(x,x')\gamma^0\gamma^5] = -\frac{1}{2}\sum_{p}\sum_{r,s=\pm} e^{ip_y(y-y')+ip_z(z-z')} \times \mathrm{sgn}(qB_z) s f^{\pm}_{ps}(t) f^{\pm}_{ps}(t')^{*} \times r g_{pr}(x) g_{pr}(x'), \quad (41)$$

$$\mathrm{tr}[S^{\pm}(x,x')\gamma^5] = \mp\sum_{p}\sum_{r,s=\pm} \frac{m}{2\kappa_p} e^{ip_y(y-y')+ip_z(z-z')} \times \mathrm{sgn}(qB_z) s f^{\pm}_{ps}(t) f^{\pm}_{p-s}(t')^{*} \times r g_{pr}(x) g_{pr}(x'). \quad (42)$$

We have to evaluate these correlators at equal time ($t = t'$) with the x and y components of the direction vectors equal ($x = x'$ and $y = y'$). For reasons we explain below, we will keep z and z′ different and introduce $\Delta \equiv z - z'$.

In this situation we can perform the $p_y$ integration using the orthogonality properties of the functions $g_{ps}(x)$. This yields

$$-\frac{1}{2}\sum_{u=\pm} u\,\mathrm{tr}[S^{u}(t,\Delta)\gamma^3] = \frac{|qB_z|}{4\pi}\sum_{k=0}^{\infty}\alpha_k\int\frac{dp_z}{2\pi}e^{ip_z\Delta}\sum_{s=\pm} s|f^{+}_{ps}(t)|^2, \quad (43)$$

$$-\frac{1}{2}\sum_{u=\pm} u\,\mathrm{tr}[S^{u}(t,\Delta)\gamma^0\gamma^5] = \frac{qB_z}{4\pi}\int\frac{dp_z}{2\pi}e^{ip_z\Delta}\sum_{s=\pm} s|f^{+}_{ps}(t)|^2\Big|_{k=0}, \quad (44)$$

$$-\frac{1}{2}\sum_{u=\pm} u\,\mathrm{tr}[S^{u}(t,\Delta)\gamma^5] = \mathrm{sgn}(m)\frac{qB_z}{4\pi}\int\frac{dp_z}{2\pi}e^{ip_z\Delta}\sum_{s=\pm} s f^{+}_{ps}(t) f^{+}_{p-s}(t)^{*}\Big|_{k=0}, \quad (45)$$

where $\alpha_k = 1$ for $k = 0$ and $\alpha_k = 2$ for $k > 0$. We have made use of Eqs. (20) and (21) to express all results in terms of particle wave functions $f^{+}_{ps}(t)$.

The quantities we will compute can be obtained from Eqs. (43)–(45) in the limit $\Delta \to 0$. Naively putting $\Delta = 0$ will not give a well-defined result, due to the presence of ultraviolet divergences. Therefore we have to regularize our expressions. For consistency, this regularization should be performed in a gauge invariant way.

A natural way to achieve this is by using the point-split regularization [24]. Instead of evaluating the two-point functions at $z = z'$ one computes them at $z - z' \equiv \Delta$ and integrates them over a distribution $h(\Delta)$. This distribution has to be normalized to unity, and should be sharply peaked around $\Delta = 0$. We will choose $h(\Delta) = \exp(-\Delta^2/4\epsilon)/(2\sqrt{\pi\epsilon})$ and take the limit $\epsilon \to 0$.

In order to maintain gauge invariance, the correlators $S^{\pm}(t,\Delta)$ have to be augmented by a gauge link $U$ connecting $z$ with $z'$. This gauge link is for both $S^{+}(t,\Delta)$ and $S^{-}(t,\Delta)$ given by

$$U(t,\Delta) = \exp\Big[iq\int_{z'}^{z} dx^{\mu}A_{\mu}(x)\Big] = \exp[-iqA_z(t)\Delta]. \quad (46)$$

Summarizing, the full point-split regularization prescription reads

$$\mathrm{tr}_r[S^{\pm}(t)\Gamma] = \lim_{\epsilon\to 0}\int d\Delta h(\Delta) U(t,\Delta)\mathrm{tr}[S^{\pm}(t;\Delta)\Gamma]; \quad (47)$$

here the subscript $r$ stands for "regularized."

We will now apply this regularization prescription to Eqs. (43)–(45) to evaluate the current density, chirality density and pseudoscalar condensate. The integral over $\Delta$ can be performed exactly giving

$$j_z(t) = \lim_{\epsilon\to 0} q\frac{|qB_z|}{2\pi}\sum_{k=0}^{\infty}\alpha_k\int\frac{dp_z}{2\pi}\,e^{-\epsilon[p_z-qA_z(t)]^2} \times[|f^+_{p+}(t)|^2-1], \tag{48}$$

$$n_5(t) = \lim_{\epsilon\to 0}\frac{qB_z}{2\pi}\int\frac{dp_z}{2\pi}\,e^{-\epsilon[p_z-qA_z(t)]^2}\times[|f^+_{p+}(t)|^2_{k=0}-1], \tag{49}$$

$$\eta(t) = \lim_{\epsilon\to 0} i\,\mathrm{sgn}(m)\frac{qB_z}{4\pi}\int\frac{dp_z}{2\pi}\,e^{-\epsilon[p_z-qA_z(t)]^2} \times\sum_{s=\pm}sf^+_{ps}(t)f^+_{p-s}(t)^*\Big|_{k=0}, \tag{50}$$

where we used that from Eq. (21) it follows that $\sum_s|f^+_{ps}(t)|^2 = 2(|f^+_{p+}(t)|^2-1)$. In the absence of a regulator and in the limit of vanishing magnetic field, Eq. (48) agrees with the results obtained in Ref. [25].

We can now verify the axial anomaly relation. In the massless limit one can show that $|f^+_{p+}(t)|^2_{k=0}-1 = -\mathrm{sgn}(p_z)$. We can now perform the $p_z$ integral in Eq. (49) in the limit $\epsilon\to 0$ giving

$$n_5(t) = -\frac{q^2}{2\pi^2}B_zA_z(t). \tag{51}$$

Taking the derivative with respect to time in the last equation gives the axial anomaly relation for massless particles in parallel electric and magnetic fields:

$$\frac{dn_5(t)}{dt} = \frac{q^2}{2\pi^2}B_zE_z(t). \tag{52}$$

If the fermions are massive the anomaly relation contains an additional term proportional to the pseudoscalar condensate. To obtain the anomaly relation in this case we will perform the time derivative on the chirality given in Eq. (49) explicitly. The limiting procedure $\epsilon\to 0$ is equivalent to performing the integration over $p_z$ in an interval symmetric around $p_z = qA_z(t)$. Therefore

$$n_5(t) = \lim_{\Lambda\to\infty}\frac{qB_z}{2\pi}\int_{-\Lambda+qA_z(t)}^{\Lambda+qA_z(t)}\frac{dp_z}{2\pi}[|f^+_{p+}(t)|^2_{k=0}-1]. \tag{53}$$

The time derivative of $n_5(t)$ contains a part arising from the integration boundaries and a part from the derivative on the wave functions. It follows directly from Eq. (17) that

$$\partial_t|f_{p+}(t)|^2 = i\kappa_p\sum_{s=\pm}sf^+_{ps}(t)f^+_{p-s}(t)^*. \tag{54}$$

Also we will use that $\kappa_p|_{k=0} = |m|$. Furthermore, for large $p_z$ one can neglect $qA_z(t)$, and from Eq. (23) it can be shown that $\lim_{p_z\to\infty}|f_{p+}(t)|^2 = 0$ and $\lim_{p_z\to-\infty}|f_{p+}(t)|^2 = 2$. By using Eq. (50) and applying the time derivative to the integration boundaries it follows that

$$\frac{dn_5(t)}{dt} = 2m\eta(t)+\frac{q^2}{2\pi^2}B_zE_z(t), \tag{55}$$

which is exactly the anomaly relation in the presence of mass.

Let us now consider a sudden switch-on electric field of the form $E(t) = E_z\theta(t)$. We discuss the functions $f^{\pm}_{ps}(t)$ in this field in Appendix B. We can only compute the induced current density and the chirality density analytically in the large $t$ limit. Applying Eq. (B13) we find that for large $t$

$$\begin{aligned}\frac{dj_z(t)}{dt} &= q\frac{|qB_z|qE_z}{2\pi^2}\,e^{-\frac{\pi m^2}{|qE_z|}}\sum_{k=0}^{\infty}\alpha_k e^{-2\pi k\frac{|qB_z|}{qE_z}}\\ &= q\frac{|qB_z|qE_z}{2\pi^2}\coth\left(\left|\frac{B_z}{E_z}\right|\pi\right)e^{-\frac{\pi m^2}{|qE_z|}},\end{aligned} \tag{56}$$

$$\frac{dn_5(t)}{dt} = \frac{q^2E_zB_z}{2\pi^2}\,e^{-\frac{\pi m^2}{|qE_z|}}. \tag{57}$$

Since these results are obtained for large $t$ in a sudden switch-on electric field, they are exact in a constant electric field.

The result Eq. (56) was derived analytically in a different way in Ref. [26]. It was also proved to be correct numerically in Ref. [27]. The result is easy to understand starting from the production rate of fermion-antifermion pairs in parallel homogeneous electric and magnetic fields [10]. That rate per unit volume equals [22,28] (see also Refs. [29–31])

$$\Gamma = \frac{q^2E_zB_z}{4\pi^2}\coth\left(\frac{B_z}{E_z}\pi\right)\exp\left(-\frac{m^2\pi}{|qE_z|}\right). \tag{58}$$

For $B_z = 0$ this rate reduces to the pair production rate in a homogeneous electric field [1,32]. The production of pairs gives rise to a homogeneous current density that has to point in the z direction because of symmetry reasons. The particles are accelerated continuously by the electric field. Therefore, at some point they will reach (almost) the speed of light. Hence, every time a pair is created the current will eventually grow by twice the charge of the fermion. So therefore the rate of change of the current density is given by $\partial_t j_z = 2q\Gamma\mathrm{sgn}(qE_z)$. Inserting Eq. (58) we see that we exactly recover Eq. (56). One can also use this argument in the opposite order, in order to derive the pair production rate from the calculation of the current density.

The result Eq. (57) generalizes the well-known production rate of chirality in parallel electric and magnetic fields for massless fermions to massive fermions. We are unaware of an earlier derivation of this result. The mass suppresses the production of chirality. By combining Eq. (57) with Eq. (55) we find that the pseudoscalar condensate in static, homogenous and parallel electric and magnetic fields equals

$$\eta(t) = \frac{q^2E_zB_z}{4\pi^2m}(e^{-\frac{\pi m^2}{|qE_z|}}-1). \tag{59}$$

## IV. LINEAR RESPONSE TO MAGNETIC FIELD

In the previous section we have considered a time-dependent electric field and a constant magnetic field that were both pointing in the z direction. To this field configuration we will now add a time-dependent magnetic field in the y direction, denoted by $B_{\mathrm{y}}(t)$. This magnetic field will be accompanied by a perpendicular electric field as can be seen from Faraday's law, $\boldsymbol{\nabla}\times\boldsymbol{E}=-\partial\boldsymbol{B}(t)/\partial t$. The additional magnetic field will induce a current density in the y direction. In this section we will compute this current density to first order in $B_{\mathrm{y}}(t)$ using linear response theory. In the next section we will use this result to study the chiral magnetic effect.

Let us write the full electromagnetic field as $A^{\mu}(x)=\bar{A}^{\mu}(x)+\tilde{A}^{\mu}(x)$. Here $\bar{A}^{\mu}(x)$ denotes the background field, consisting of the electric and magnetic fields pointing in the z direction. The field $\tilde{A}^{\mu}(x)$ denotes the perturbation on this background, which in this case is the magnetic field in the y direction with its corresponding perpendicular electric field.

From linear response theory it follows that to first order in $\tilde{A}_{\mu}(x)$ the induced current density in the electromagnetic field $A^{\mu}(x)$ equals $j^{\mu}(x)=j^{\mu}_{\bar{A}}(x)=j^{\mu}_{\bar{A}}(x)+\delta j^{\mu}_{\bar{A},\tilde{A}}(x)$ where

$$\delta j^{\mu}_{\bar{A},\tilde{A}}(x)=\int \mathrm{d}^4x'\,\Pi^{\mu\nu}_{\mathrm{R}}(x,x')\tilde{A}_{\nu}(x'). \tag{60}$$

Here the retarded current-current correlator (or equivalently photon polarization tensor) in the background field $\bar{A}_{\mu}(x)$ is given by $\Pi^{\mu\nu}_{\mathrm{R}}(x,x')=\Pi^{\mu\nu}_{\mathrm{C}}(x,x')\theta(t-t')$ with

$$\Pi^{\mu\nu}_{\mathrm{C}}(x,x')=-\mathrm{i}q^2\langle 0|[\bar{\Psi}(x)\gamma^{\mu}\Psi(x),\bar{\Psi}(x')\gamma^{\nu}\Psi(x')]|0\rangle. \tag{61}$$

Using Eqs. (25) and (37) we can express $\Pi^{\mu\nu}_{\mathrm{C}}(x,x')$ as

$$\Pi^{\mu\nu}_{\mathrm{C}}(x,x')=-\mathrm{i}q^2\sum_{u=\pm}u\,\mathrm{tr}[\gamma^{\mu}S^{u}(x,x')\gamma^{\nu}S^{-u}(x',x)], \tag{62}$$

where $S^{\pm}(x,x')$ is the two-point correlation function in the background field, given explicitly in Eq. (38).

Since the background electric and magnetic fields are both pointing in the z direction, they cannot solely induce a current in the y direction. As a result $j^{\mathrm{y}}_{\bar{A}}(t)=0$. Hence the induced current density in the y direction can only arise from the perturbation and is therefore of the following form:

$$j_{\mathrm{y}}(t)=\int_{-\infty}^{t}\mathrm{d}t'H(t,t')B_{\mathrm{y}}(t'), \tag{63}$$

where $H(t,t')$ can be obtained from $\Pi^{\mu\nu}_{\mathrm{C}}(x,x')$ as we will explain in more detail below. The photon polarization tensor in an electric plus magnetic background has been studied by other authors before in different contexts [33]. Furthermore, the photon polarization tensor in a purely magnetic background has been studied in detail in several works [34], for recent analyses and applications we refer to [5,35].

In the following subsections we will compute the function $H(t,t')$ in two cases, labeled by A and B. In case A we will take the only nonvanishing component of the perturbation field to be $\tilde{A}_{\mathrm{z}}(x)=-B_{\mathrm{y}}(t)\mathrm{x}$. In case B the only nonvanishing component is chosen as $\tilde{A}_{\mathrm{x}}(x)=B_{\mathrm{y}}(t)\mathrm{z}$. These two cases lead to the same magnetic field in the y direction, $B_{\mathrm{y}}(t)$, but give rise to different perpendicular electric fields. The only nonvanishing component of the additional electric field is in the first case $E_{\mathrm{z}}=\partial_t B_{\mathrm{y}}(t)\mathrm{x}$, and in the second case $E_{\mathrm{x}}=-\partial_t B_{\mathrm{y}}(t)\mathrm{z}$. By taking the average of the two cases, one obtains a more symmetric electric field, which is circular in the x–z plane.

If $B_{\mathrm{y}}(t)$ is constant in time, the perpendicular electric field vanishes and the two cases are gauge equivalent. However, we do not know how to implement a constant magnetic field exactly in a practical numerical calculation. In the numerical evaluation of Eq. (63) one might replace the lower integration bound by a finite time $t_a$. But then one effectively deals with a sudden switch-on perpendicular field of the following form:

$$B_{\mathrm{y}}(t)=\begin{cases}0 & \text{if } t<t_a,\\ B_{\mathrm{y}} & \text{if } t\geq t_a.\end{cases} \tag{64}$$

This sudden switch-on leads to large perpendicular electric fields, and as a result the current densities in cases A and B can be different. To instead implement a magnetic field that is effectively constant in time we have to switch it on slowly. In our numerical calculations we will take a magnetic field of the following form:

$$B_{\mathrm{y}}(t)=\begin{cases}0 & \text{if } t<t_a,\\ B_{\mathrm{y}}(t-t_a)/(t_b-t_a) & \text{if } t_a\leq t\leq t_b,\\ B_{\mathrm{y}} & \text{if } t>t_b.\end{cases} \tag{65}$$

If we choose $t_b-t_a$ large enough and $t_b$ small enough before the important physical effects happen, the magnetic field is effectively constant. In that situation the perpendicular electric fields are small and the induced current density in cases A and B should approximately have the same magnitude. We will use this feature to test our methodology.

### A. $\tilde{A}_{\mathrm{z}}(x)=-B_{\mathrm{y}}(t)\mathrm{x}$

In the case that $\tilde{A}_{\mathrm{z}}(x)=-B_{\mathrm{y}}(t)\mathrm{x}$ we obtain

$$H(t,t')=\int \mathrm{d}^3\boldsymbol{x}'\mathrm{x}'\Pi^{23}_{\mathrm{C}}(x,x'). \tag{66}$$

After inserting the explicit expression for $S^{\pm}(x,x')$, taking the trace, and integrating over y, z, $p'_{\mathrm{y}}$ and $p'_{\mathrm{z}}$ we find

$$H(t,t') = -q^2 \sum_{\boldsymbol{p}} \sum_{k'=0}^{\infty} \int_{-\infty}^{\infty} \mathrm{d}x' x' \times \left[ \frac{\lambda_{\boldsymbol{p}}}{\kappa_{\boldsymbol{p}}} V_{\boldsymbol{p},\boldsymbol{p}'}(t,t') W_{\boldsymbol{p},\boldsymbol{p}'}(\mathrm{x},\mathrm{x}') \right]_{p_y'=p_y, p_z'=p_z}, \quad (67)$$

where the functions $V$ and $W$ are given by

$$V_{\boldsymbol{p},\boldsymbol{p}'}(t,t') = \mathrm{Im} \sum_{s=\pm} s f^+_{\boldsymbol{p}s}(t) f^+_{\boldsymbol{p}'s}(t) f^+_{\boldsymbol{p}-s}(t')^* f^+_{\boldsymbol{p}'s}(t')^*, \quad (68)$$

$$W_{\boldsymbol{p},\boldsymbol{p}'}(\mathrm{x},\mathrm{x}') = \sum_{s=\pm} g_{\boldsymbol{p}-s}(\mathrm{x}) g_{\boldsymbol{p}'s}(\mathrm{x}) g_{\boldsymbol{p}s}(\mathrm{x}') g_{\boldsymbol{p}'s}(\mathrm{x}'). \quad (69)$$

The expression for $H(t,t')$ can be simplified by performing the integration over $\mathrm{x}'$ followed by integration over $p_y$. Using the relations from Appendix A it can be shown that

$$\int_{-\infty}^{\infty} \frac{\mathrm{d}p_y}{2\pi} \int_{-\infty}^{\infty} \mathrm{d}x' x' W_{\boldsymbol{p},\boldsymbol{p}'}(\mathrm{x},\mathrm{x}') \Big|_{p_y'=p_y} = \frac{\sqrt{|qB_z|}}{2\pi\sqrt{2}} \sqrt{k} [2\delta_{k,k'} - \delta_{k-1,k'} - \delta_{k+1,k'}]. \quad (70)$$

Inserting Eq. (70) into Eq. (67) yields

$$H(t,t') = \frac{q^2}{2\pi} \sum_{k=1}^{\infty} \int_{-\infty}^{\infty} \frac{\mathrm{d}p_z}{2\pi} \omega_k \times [2V_{k,k}(t,t') - V_{k,k-1}(t,t') - V_{k,k+1}(t,t')]_{p_z=p_z'}, \quad (71)$$

where

$$\omega_k = \frac{|qB_z|k}{\sqrt{2|qB_z|k + m^2}}. \quad (72)$$

To speed up the numerical computation it is convenient to take the wave functions with the same momenta together in the integrand. For this reason we rewrite Eq. (71) into

$$H(t,t') = -\frac{q^2}{2\pi} \int_{-\infty}^{\infty} \frac{dp_z}{2\pi} \omega_1 V_{1,0}(t,t') + \frac{q^2}{2\pi} \sum_{k=1}^{\infty} \int_{-\infty}^{\infty} \frac{dp_z}{2\pi} \times [2\omega_k V_{k,k}(t,t') - \omega_{k+1} V_{k+1,k}(t,t') - \omega_k V_{k,k+1}(t,t')]_{p_z=p_z'}. \quad (73)$$

### B. $\tilde{A}_x(x) = B_y(t)z$

If $\tilde{A}_x(x) = B_y(t)z$ we obtain

$$H(t,t') = -\int \mathrm{d}^3 \boldsymbol{x}' z' \Pi_C^{21}(x,x'). \quad (74)$$

Inserting the explicit expression for the two-point function and performing the trace, we find that

$$\Pi_C^{21}(x,x') = \mathrm{i} \frac{q^2}{2} \sum_{\boldsymbol{p},\boldsymbol{p}'} e^{\mathrm{i}(p_y - p_y')(y-y') + \mathrm{i}(p_z - p_z')(z-z')} \times \left\{ W^A_{\boldsymbol{p},\boldsymbol{p}'}(\mathrm{x},\mathrm{x}') \left[ V^A_{\boldsymbol{p},\boldsymbol{p}'}(t,t') + \frac{m^2}{\kappa_{\boldsymbol{p}}\kappa_{\boldsymbol{p}'}} V^B_{\boldsymbol{p},\boldsymbol{p}'}(t,t') \right] + \frac{\lambda_{\boldsymbol{p}}\lambda_{\boldsymbol{p}'}}{\kappa_{\boldsymbol{p}}\kappa_{\boldsymbol{p}'}} W^B_{\boldsymbol{p},\boldsymbol{p}'}(\mathrm{x},\mathrm{x}') V^B_{\boldsymbol{p},\boldsymbol{p}'}(t,t') \right\}, \quad (75)$$

where we have defined the following functions:

$$V^A_{\boldsymbol{p},\boldsymbol{p}'}(t,t') = \mathrm{Im} \sum_{s=\pm} f^+_{\boldsymbol{p}s}(t) f^+_{\boldsymbol{p}'s}(t) f^+_{\boldsymbol{p}s}(t')^* f^+_{\boldsymbol{p}'s}(t')^*, \quad (76)$$

$$V^B_{\boldsymbol{p},\boldsymbol{p}'}(t,t') = \mathrm{Im} \sum_{s=\pm} f^+_{\boldsymbol{p}s}(t) f^+_{\boldsymbol{p}'s}(t) f^+_{\boldsymbol{p}-s}(t')^* f^+_{\boldsymbol{p}'-s}(t')^*, \quad (77)$$

$$W^A_{\boldsymbol{p},\boldsymbol{p}'}(\mathrm{x},\mathrm{x}') = \sum_{s=\pm} s g_{\boldsymbol{p}s}(\mathrm{x}) g_{\boldsymbol{p}'-s}(\mathrm{x}) g_{\boldsymbol{p}s}(\mathrm{x}') g_{\boldsymbol{p}'-s}(\mathrm{x}'), \quad (78)$$

$$W^B_{\boldsymbol{p},\boldsymbol{p}'}(\mathrm{x},\mathrm{x}') = \sum_{s=\pm} s g_{\boldsymbol{p}s}(\mathrm{x}) g_{\boldsymbol{p}'-s}(\mathrm{x}) g_{\boldsymbol{p}-s}(\mathrm{x}') g_{\boldsymbol{p}'s}(\mathrm{x}'). \quad (79)$$

To simplify $H(t,t')$ we can make use of the following relation:

$$\int \frac{\mathrm{d}p_z}{2\pi} \int \frac{\mathrm{d}p_z'}{2\pi} \int \mathrm{d}z' z' \mathrm{e}^{\mathrm{i}(p_z - p_z')(z-z')} f(p_z, p_z') = -\mathrm{i} \int \frac{\mathrm{d}\bar{p}_z}{2\pi} \left[ \frac{\partial}{\partial h} \mathrm{e}^{\mathrm{i}zh} f(\bar{p}_z + h/2, \bar{p}_z - h/2) \right]_{h=0}. \quad (80)$$

Furthermore, using the relations from Appendix A it follows that

$$\int_{-\infty}^{\infty} \frac{\mathrm{d}p_y}{2\pi} \int_{-\infty}^{\infty} \mathrm{d}x' W^A_{\boldsymbol{p},\boldsymbol{p}'}(\mathrm{x},\mathrm{x}') \Big|_{p_y'=p_y} = \frac{|qB_z|}{2\pi} (\delta_{k+1,k'} - \delta_{k-1,k'}), \quad (81)$$

$$\int_{-\infty}^{\infty} \frac{\mathrm{d}p_y}{2\pi} \int_{-\infty}^{\infty} \mathrm{d}x' W^B_{\boldsymbol{p},\boldsymbol{p}'}(\mathrm{x},\mathrm{x}') \Big|_{p_y'=p_y} = 0. \quad (82)$$

Using the last three equations above we find

$$H(t,t') = -\frac{q^2|qB_z|}{2\pi} \sum_{k=0}^{\infty} \int \frac{\mathrm{d}\bar{p}_z}{2\pi} \frac{\partial}{\partial h} \times \left[ V^A_{k,k+1}(t,t') + \frac{m^2}{\kappa_k \kappa_{k+1}} V^B_{k,k+1}(t,t') \right], \quad (83)$$

where $p_z = \bar{p}_z + h/2$ and $p_z' = \bar{p}_z - h/2$.

### C. Numerical procedure

We now will discuss the details of the numerical evaluation of the current density along the perpendicular magnetic field. Firstly, we obtain the wave functions $f^+_{\boldsymbol{p}s}(t)$ numerically through solving Eqs. (17) and (18) using a

Runge-Kutta method implemented in MATLAB. We make sure that we obtain $f^{+}_{ps}(t)$ at equally spaced time steps. The next step is to construct the integrand of Eqs. (73) and (83) for different $t'$. The derivative in the integrand of Eq. (83) is computed using finite differences. We then perform the $t'$ integration in Eq. (63) using the trapezoidal rule with a lower integration cutoff. Thereafter we perform the $p_z$ integral, in an interval symmetric around $p_z = 0$, using the trapezoidal rule. The upper and lower cutoff are taken so large that varying them does not change the results. The last step is to perform the sum over $k$. The results are dominated by the small $k$ values; therefore we sum over $k$ until we reach convergence. Typically one only has to sum over a few values of $k$ to obtain an accurate answer.

## V. RESULTS

We will now study the current density generated by the chiral magnetic effect in parallel electric and magnetic fields with a perpendicular magnetic field as in Fig. 1. We will compute this current density numerically using the linear response relation Eq. (63). Since the calculation is based on linear response, our results will be valid for perpendicular magnetic fields that are small compared to the parallel electric and magnetic fields.

The full electromagnetic current density has two components. Firstly, it has a component along the perpendicular magnetic field due to the chiral magnetic effect. Secondly, it has a component in the longitudinal direction along the electric and magnetic field due to pair production. This component does not vanish for weak perpendicular magnetic fields, and can to first order be computed using Eq. (48). As explained in the introduction the longitudinal component vanishes in the QCD setup due to a cancellation of the contribution of red and green quarks.

The electromagnetic current density will generate fields themselves which can modify the dynamics. This backreaction can be safely neglected as long as the fields induced by the currents stay small compared to the background fields. Such regime can always be reached by considering times shortly after the switch-on of the background fields. In this article we will not consider this backreaction and leave its study for future work.

We will present results for the chiral magnetic effect in a sudden switch-on electric field and a pulsed electric field below. We consider a perpendicular magnetic field that is effectively constant in time as in Eq. (65). The formalism we have developed in this article allows one to analyze the chiral magnetic effect in other settings as well.

We have performed all numerical calculations in an effectively constant magnetic field using both gauge field choices A and B. These choices are approximately gauge equivalent, and the accuracy of the approximation can be improved by switching on the effectively constant magnetic field more slowly. The calculations performed using gauge field choices A and B are independent and hence can be used to test our methodology. In the numerical calculations in an effectively constant magnetic field we have found excellent agreement between the results obtained with choices A and B.

### A. Sudden switch-on electric field

Here we will consider the chiral magnetic effect in a sudden switch-on electric field of the form $E(t) = E_z\theta(t)$. The corresponding gauge field reads $A_z(t) = -E_z\theta(t)t$. The perpendicular magnetic field is taken to be effectively constant. In Ref. [10], the current density in the y direction was computed exactly for $t \gg 0$. For small $B_y$ and $t \gg 0$ the rate of current density generation equals [10]

$$\partial_t j_y = \frac{q^2 B_y}{2\pi^2} \frac{|qE_z|B_z^2}{B_z^2 + E_z^2} \coth\left(\frac{B_z}{E_z}\pi\right) \exp\left(-\frac{m^2\pi}{|qE_z|}\right). \quad (84)$$

In order to cancel the rapid oscillations in the current density arising from the sudden switch-on of the electric field we will investigate the running average of the current density, here defined as

$$\langle j_y(t)\rangle = \int_{t-c/\sqrt{|qE_z|}}^{t+c/\sqrt{|qE_z|}} \mathrm{d}t' j_y(t'). \quad (85)$$

We display the results of the numerical computation of the running average of the current density using $c = 1$ in Fig. 2 for different values of $\tilde{m} = m/\sqrt{|qE_z|}$ and $B_z/E_z = 1$. The linear response calculation shows that after the switch-on the current quickly grows linear with time. A fermion mass suppresses the production of chirality as can be seen from Eq. (57). This explains why the current density is smaller for particles with a larger mass.

In Fig. 3 we compare our numerical results for the rate of current density generation to the small $B_y$ limit of the exact result, given in Eq. (84). It can be seen that we find excellent agreement between the results obtained using

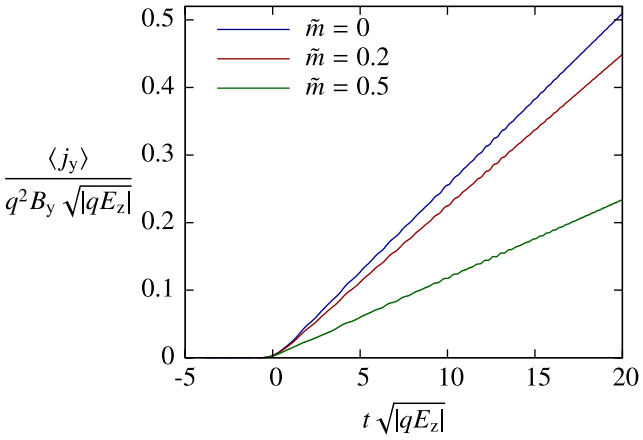


FIG. 2 (color online). Running average of the current density generated by the chiral magnetic effect in an electric field suddenly switched on at $t = 0$. Here $B_z/E_z = 1$.

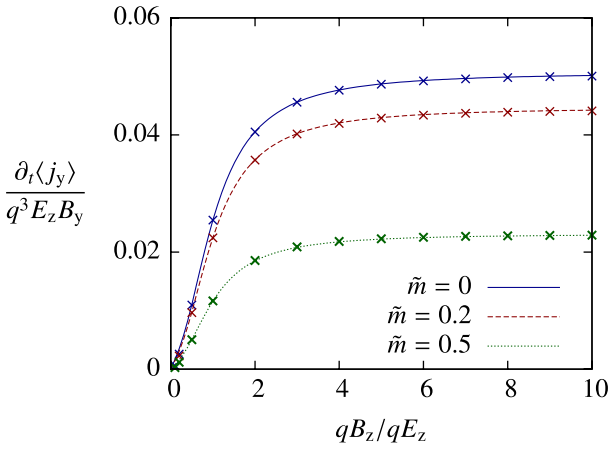


FIG. 3 (color online). Rate of current density generation due to the chiral magnetic effect at late times in a sudden switch-on electric field as a function of $B_z/E_z$ for different masses. The lines denote the small $B_y$ limit of the exact result; points indicate the results of the numerical calculations using linear response.

linear response and the small $B_y$ limit of the exact result. Thus our linear response approach has passed a critical test. It implies that the study of the dynamics of the chiral magnetic effect using linear response can be performed successfully. Alternatively, our results can be seen as an independent verification of the results obtained in Ref. [10].

It can be seen that the rate of current density generation increases if $B_z$ is enlarged. This is natural, since the amount of chirality production is increased. But at the same time enlarging $B_z$ decreases the degree of polarization of the fermions in the y direction. The combination of these two effects results in the saturation of the rate of current generation for large $B_z$.

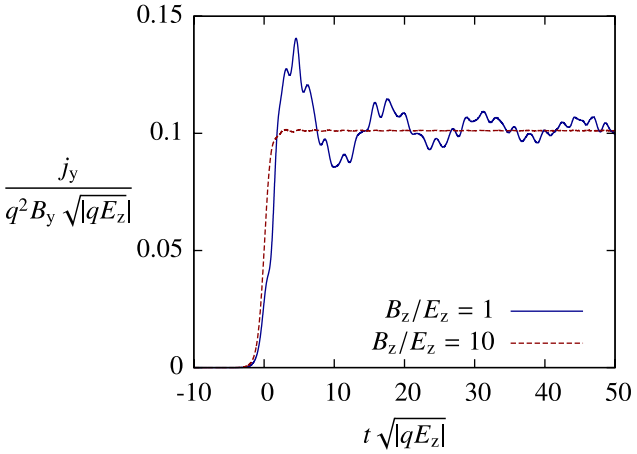


FIG. 4 (color online). Current density due to the chiral magnetic effect in a pulsed electric field, as a function of time. Here $\tau = 1/\sqrt{|qE_z|}$ and $\tilde{m} = 0$.

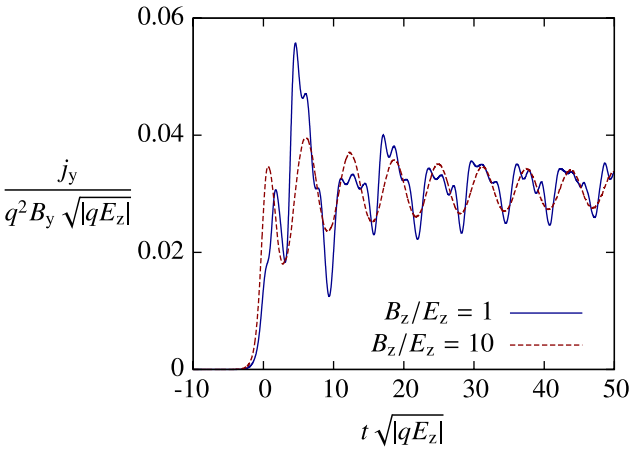


FIG. 5 (color online). Same as in Fig. 4 but now for $\tilde{m} = 0.5$.

### B. Pulsed electric field

We will now study the chiral magnetic effect in a pulsed electric field that has the form $E_z(t) = E_z/\cosh^2(t/\tau)$. The corresponding gauge field reads $A_z(t) = -E_z[1 + \tanh(t/\tau)]\tau$. The perpendicular magnetic field is taken to be effectively constant.

In Figs. 4 and 5 we display the current density generated by the chiral magnetic effect as a function of time for $\tau = 1/\sqrt{|qE_z|}$ and respectively $\tilde{m} = m/\sqrt{|qE_z|} = 0$ and $\tilde{m} = 0.5$. It can be seen that the current density rises quickly around $t = 0$. This is because only then an electric field is present so that chirality will be produced. For large $t$ the current does not grow anymore because the production of chirality has stopped. For large values of $B_z/E_z$ we find that the current density becomes approximately constant in time if $\tilde{m} = 0$. If the fermions are massive the current density exhibits a slowly damped sinusoidal oscillation for large values of $B_z/E_z$. The mass also suppresses the magnitude of the current.

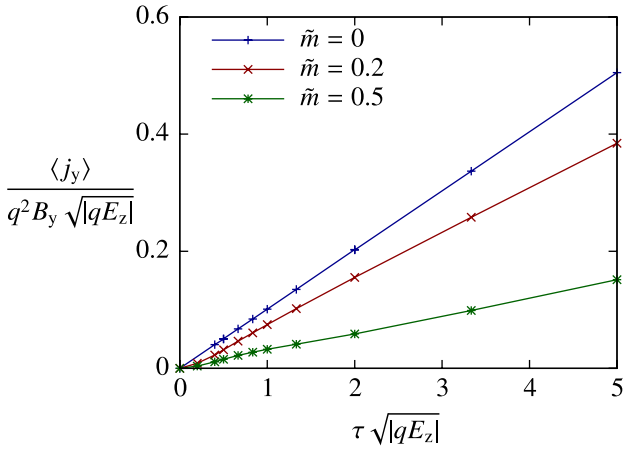


FIG. 6 (color online). Average current density at late times in a pulsed electric field as a function of $\tau$ for different $\tilde{m}$.

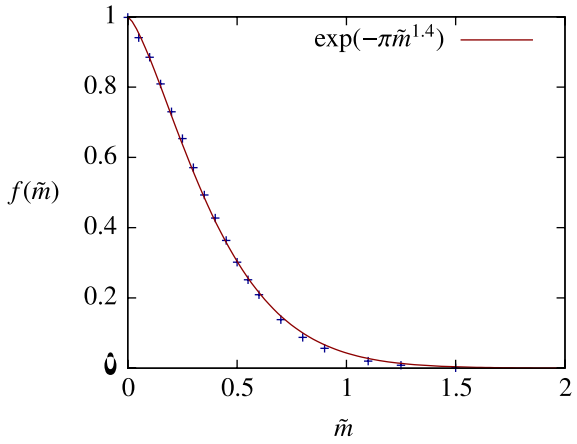


FIG. 7 (color online). The function $f(\tilde{m})$ which describes the mass dependence of the average current density at late times in a pulsed electric field. Points are numerical results; a solid line is a fit.

We observe that for smaller values of $B_z/E_z$ the current density oscillates around the behavior of the current density at large $B_z/E_z$. Therefore the running average of the current density seems to be independent of $B_z/E_z$. To investigate the dependence on $\tau$ we have displayed the running average of the current density at late times in Fig. 6 for $B_z/E_z = 10$. We find that the running average increases linear with $\tau$. Through observation of our numerical results we find that for all values of $B_z/E_z$ the running average of the current density at late times is summarized by the following formula:

$$\langle j_y \rangle = \frac{q^2|q|\tau}{\pi^2} B_y E_z f(\tilde{m}) \mathrm{sgn}(B_z), \tag{86}$$

where we have displayed $f(\tilde{m})$ for different values of $\tilde{m}$ in Fig. 7. We find a reasonable fit to our data with the function $f(\tilde{m}) = \exp(-\pi\tilde{m}^{1.4})$.

## VI. CONCLUSIONS

In this article we have investigated the real-time dynamics of the chiral magnetic effect using linear response theory. We have considered a field configuration in which a homogeneous (chromo)electric field with arbitrary time dependence lies parallel to a homogeneous and static (chromo)magnetic field. These parallel fields are the source of the chirality. To this field configuration we have added a perpendicular homogeneous and static magnetic field. We have computed the induced current density along this perpendicular magnetic field explicitly for a sudden switch-on and a pulsed electric field.

In the sudden switch-on electric field we have obtained excellent agreement with an earlier independent analytic computation of the current density. In the pulsed electric field we could summarize the induced current density that we have obtained numerically with a simple analytic formula.

The main purpose of this article was to demonstrate the dynamics of the chiral magnetic effect using linear response theory. We hope that our results will be extended to other interesting field configurations in the future. For example, in heavy ion collisions it would be important to answer the question of whether there is enough time for the chiral magnetic effect to occur in the quickly decaying magnetic field. This question could be addressed using our methodology. The chiral magnetic effect could also be investigated with lasers that create strong electromagnetic fields. For that purpose it would be important to extend the results to field configurations that are as close to the experimental situation as possible.

As a side result of our work we have obtained a derivation of the induced current density in static homogeneous parallel electric and magnetic fields. We have also obtained an analytic formula for the chirality production for massive fermions in static homogeneous parallel electric and magnetic fields.

## ACKNOWLEDGMENTS

I would like to thank Gerald Dunne, Kenji Fukushima, Dmitri Kharzeev, Larry McLerran and Vladimir Skokov for discussions. The work of H. J. W. was supported by the Extreme Matter Institute (EMMI) and by the Alexander von Humboldt Foundation.

## APPENDIX A: RELATIONS INVOLVING THE FUNCTION $g_{ps}(x)$

To evaluate these integrals we will make use of the following four identities which directly follow from the properties of the Hermite polynomials:

$$\int_{-\infty}^{\infty} dx' x' g_{ps}(x') g_{p's}(x') \Big|_{p_y'=p_y} = \frac{p_y}{qB_z}\delta_{k,k'}(1-\delta_{k,0}\delta_{s-}) + \frac{1}{\sqrt{2|qB_z|}}(\sqrt{k}\delta_{k-s,k'} + \sqrt{k+s}\delta_{k+s,k'}), \tag{A1}$$

$$\frac{1}{qB_z}\int_{-\infty}^{\infty}\frac{dp_y}{2\pi} p_y g_{p-s}(x) g_{p's}(x) \Big|_{p_y'=p_y} = \frac{|qB_z|}{2\pi}\Big[x\delta_{k-s,k'} - \frac{1}{\sqrt{2|qB_z|}} \times (\sqrt{k-s}\delta_{k-2s,k'} + \sqrt{k}\delta_{k,k'})\Big], \tag{A2}$$

$$\int_{-\infty}^{\infty}\frac{dp_y}{2\pi} g_{p-s}(x) g_{p's}(x) \Big|_{p_y'=p_y} = \frac{|qB_z|}{2\pi}\delta_{k-s,k'}. \tag{A3}$$

$$\int_{-\infty}^{\infty} \mathrm{d}x g_{\boldsymbol{p}s}(x) g_{\boldsymbol{p}'-s}(x) \Big|_{p_y'=p_y} = \delta_{k+s,k'}. \tag{A4}$$

## APPENDIX B: WAVE FUNCTIONS IN A SUDDEN SWITCH-ON ELECTRIC FIELD

We will review the explicit solutions for the wave functions $f^{\pm}_{\boldsymbol{p}s}(t)$ for a sudden switch-on electric field of the form $E(t) = E_z\theta(t)$ [22]. Then we will evaluate an integral that is necessary for computing the induced current and chirality production.

For the sudden switch-on electric field we have $A_z(t) = -E_z t\theta(t)$. For $t < 0$ we can use the wave functions in vanishing electromagnetic field, given in Eq. (23). If $t > 0$ the electric field is no longer vanishing. It follows from combining Eqs. (17) and (18) that $f^{\pm}_{\boldsymbol{p}s}(t)$ then satisfies

$$\left[-\partial_t^2 - q^2E_z^2\left(t + \frac{p_z}{qE_z}\right)^2 + \mathrm{i}sqE_z\right] f^{\pm}_{\boldsymbol{p}s}(t) = \kappa^2 f^{\pm}_{\boldsymbol{p}s}(t). \tag{B1}$$

Equation (B1) is an eigenvalue equation for a particle in an upside-down harmonic potential. There are no bound states, so $\kappa$ is not quantized. The solution is a linear combination of parabolic cylinder functions $D_\nu(z)$,

$$f^{\pm}_{\boldsymbol{p}s}(t) = \alpha^{\pm}_s D_{\nu_s}(\xi) + \beta^{\pm}_s D_{\nu_s}(-\xi), \tag{B2}$$

where $\nu_s = -(s\,\mathrm{sgn}(qE_z) + 1 + \mathrm{i}\kappa^2/|qE_z|)/2$ and $\xi = \sqrt{2|qE_z|}\mathrm{e}^{\mathrm{i}\pi/4}(t + p_z/qE_z)$.

In the conventional normalization the parabolic cylinder functions are given explicitly by the following integrals

$$D_\nu(z) = \frac{1}{\Gamma(-\nu)}\,\mathrm{e}^{-\frac{1}{4}z^2}\int_0^\infty \mathrm{d}t\, t^{-\nu-1}\mathrm{e}^{-zt-\frac{1}{2}t^2}, \tag{B3}$$

for $\mathrm{Re}(\nu) < 0$, and

$$D_\nu(z) = \sqrt{\frac{2}{\pi}}\mathrm{e}^{\frac{1}{4}z^2}\int_0^\infty \mathrm{d}t\, t^\nu \cos\left(zt - \frac{1}{2}\pi\nu\right)\mathrm{e}^{-\frac{1}{2}t^2}, \tag{B4}$$

for $\mathrm{Re}(\nu) > -1$. Using these relations one can show that $D_\nu(0) = 2^{\nu/2}\sqrt{\pi}/\Gamma[(1-\nu)/2]$. Asymptotically the parabolic cylinder functions behave as follows:

$$\lim_{|z|\to\infty} D_\nu(z) = z^\nu \mathrm{e}^{-\frac{1}{4}z^2} - c_\nu\frac{\sqrt{2\pi}}{\Gamma(-\nu)}z^{-\nu-1}\mathrm{e}^{\frac{1}{4}z^2}, \tag{B5}$$

with $c_\nu = 0$ for $|\arg(z)| < \frac{3\pi}{4}$, $c_\nu = \exp(\mathrm{i}\pi\nu)$ for $\frac{\pi}{4} < |\arg(z)| < \frac{5\pi}{4}$, and $c_\nu = \exp(-\mathrm{i}\pi\nu)$ for $-\frac{5\pi}{4} < |\arg(z)| < -\frac{\pi}{4}$. These asymptotic functions describe the real parabolic cylinder functions very well if $|z| > 2|\nu|$.

The constants $\alpha^{\pm}_s$ and $\beta^{\pm}_s$ of Eq. (B2) can be found by requiring continuity of $f^{\pm}_{\boldsymbol{p}s}(t)$ and its derivative at $t = 0$. This gives the following two equations:

$$\alpha^{\pm}_s = \frac{1}{W}\sqrt{\frac{p_0 \mp sp_z}{p_0}}[-\mathrm{e}^{\mathrm{i}\pi/4}\sqrt{2|qE_z|}D'_{\nu_s}(-\xi_0) \pm \mathrm{i}p_0 D_{\nu_s}(-\xi_0)], \tag{B6}$$

$$\beta^{\pm}_s = \frac{1}{W}\sqrt{\frac{p_0 \mp sp_z}{p_0}}[-\mathrm{e}^{\mathrm{i}\pi/4}\sqrt{2|qE_z|}D'_{\nu_s}(\xi_0) \mp \mathrm{i}p_0 D_{\nu_s}(\xi_0)], \tag{B7}$$

where $\xi_0 = \sqrt{2}\mathrm{e}^{\mathrm{i}\pi/4}p_z/|qE_z|^{1/2}\mathrm{sgn}(qE_z)$ and $W$ denotes the Wronskian of the two independent solutions presented in Eq. (B1). Applying Abel's differential equation identity to Eq. (B2) shows that the Wronskian is independent of $\xi$. Hence without loss of generality we can evaluate $W$ at $\xi = 0$, which yields $W = 2\mathrm{e}^{\mathrm{i}\pi/4}\sqrt{\pi|qE_z|}/\Gamma(-\nu_s)$. Using the relation $D'_\nu(z) = \frac{1}{2}zD_\nu(z) - D_{\nu+1}(z)$ we can simplify Eqs. (B6) and (B7) to

$$\alpha^{\pm}_s = \frac{\Gamma(-\nu_s)}{\sqrt{2\pi}}\sqrt{\frac{p_0 \mp sp_z}{p_0}}\left[D_{\nu_s+1}(-\xi_0) + \frac{\mathrm{e}^{\mathrm{i}\pi/4}}{\sqrt{2|qE_z|}} \times (p_z\mathrm{sgn}(qE_z) \pm p_0)D_{\nu_s}(-\xi_0)\right], \tag{B8}$$

$$\beta^{\pm}_s = \frac{\Gamma(-\nu_s)}{\sqrt{2\pi}}\sqrt{\frac{p_0 \mp sp_z}{p_0}}\left[D_{\nu_s+1}(\xi_0) - \frac{\mathrm{e}^{\mathrm{i}\pi/4}}{\sqrt{2|qE_z|}} \times (p_z\mathrm{sgn}(qE_z) \pm p_0)D_{\nu_s}(\xi_0)\right]. \tag{B9}$$

Using the asymptotic expansion of the parabolic cylinder functions, Eq. (B4), it is possible to obtain a very good approximation for the function $f^{\pm}_{\boldsymbol{p}s}(t)$ away from the points $p_z = -qE_z t$ and $p_z = 0$. Let us now for a moment choose $qE_z > 0$ and take $\sqrt{|qE_z|}t \gg 1$. In order to obtain the induced current we need to evaluate $|f^{+}_{\boldsymbol{p}+}(t)|^2$, for which we find after taking the dominating terms in the asymptotic expansion and approximating $p_0$ by $|p_z|$ the following:

$$|f^{+}_{\boldsymbol{p}+}(t)|^2 \approx \begin{cases} 2 & \text{for } p_z \lesssim -qE_z t - \Delta, \\ 2\mathrm{e}^{-\frac{\pi\kappa^2}{|qE_z|}} + g(\zeta) & \text{for } -qE_z t + \Delta \lesssim p_z \lesssim -\Delta, \\ 0 & \text{for } p_z \gtrsim \Delta, \end{cases} \tag{B10}$$

where $\Delta = 2|qE_z|^{1/2}|1 + \frac{\mathrm{i}\kappa^2}{2|qE_z|}|$, $\zeta = \sqrt{|qE_z|}(t + p_z/qE_z)$, and

$$g(\zeta) = \frac{2}{\sqrt{\pi}}\frac{1}{\zeta}[\mathrm{e}^{-\frac{\pi\kappa^2}{4|qE_z|}} - \mathrm{e}^{-\frac{5\pi\kappa^2}{4|qE_z|}}] \times \mathrm{Re}\left[\Gamma\left(1 - \frac{\mathrm{i}\kappa^2}{2|qE_z|}\right)\mathrm{e}^{\mathrm{i}\zeta^2 + \frac{\mathrm{i}\kappa^2}{|qE_z|}\log|\sqrt{2}\zeta| + \mathrm{i}\pi/4}\right]. \tag{B11}$$

As follows from Eq. (48) we have to evaluate the following integral to obtain the induced current:

$$I(\kappa, t) = \lim_{\epsilon \to 0} \int_{-\infty}^{\infty} \frac{\mathrm{d}p_z}{2\pi} \, \mathrm{e}^{-\epsilon(p_z + qE_z t)^2} [|f^+_{\boldsymbol{p}^+}(t)|^2 - 1]. \tag{B12}$$

In general this integral can only be evaluated numerically. But using Eq. (B10) we can obtain $I(\kappa, t)$ exactly for large $t$. Firstly one realizes that taking the limit $\epsilon \to 0$ implies that we have to integrate $|f^+_{\boldsymbol{p}^+}(t)|^2 - 1$ over $p_z$ in an interval symmetric around $p_z = -qE_z t$. The contribution to the integral in the region where the approximation Eq. (B10) breaks down can be bounded from below and above by a time-independent constant. The contributions for $p_z < -2qE_z t$ and $p_z > 0$ will cancel each other. The nonvanishing contribution comes from the intermediate region in which $-2qE_z t < p_z < 0$. The integral over the rapidly oscillating function $g(\zeta)$ is subdominant in the large $t$ limit. The dominant contribution in the large $t$ limit is $qE_z t$ coming from the interval $-2qE_z t < p_z < -qE_z t$ and $qE_z t[2\exp(-\pi\kappa^2/|qE_z|) - 1]$ from the interval $-qE_z t < p_z < 0$. Adding both contributions yields

$$\lim_{t \to \infty} \frac{1}{t} I(\kappa, t) = \frac{qE_z}{\pi} \, \mathrm{e}^{-\frac{\pi\kappa^2}{|qE_z|}}. \tag{B13}$$

By repeating the analysis for $qE_z < 0$ one can verify that the sign of Eq. (B13) is correct, so Eq. (B13) holds for all values of $qE_z$.


[1] J. S. Schwinger, Phys. Rev. **82**, 664 (1951).
[2] S. L. Adler, Phys. Rev. **177**, 2426 (1969); J. S. Bell and R. Jackiw, Nuovo Cimento Soc. Ital. Fis. A **60**, 47 (1969).
[3] A. Vilenkin, Phys. Rev. D **22**, 3080 (1980).
[4] D. E. Kharzeev, L. D. McLerran, and H. J. Warringa, Nucl. Phys. **A803**, 227 (2008).
[5] A. Y. Alekseev, V. V. Cheianov, and J. Frohlich, Phys. Rev. Lett. **81**, 3503 (1998); K. Fukushima, D. E. Kharzeev, and H. J. Warringa, Phys. Rev. D **78**, 074033 (2008); D. E. Kharzeev and H. J. Warringa, Phys. Rev. D **80**, 034028 (2009); H.-U. Yee, J. High Energy Phys. 11 (2009) 085; A. Rebhan, A. Schmitt, and S. A. Stricker, J. High Energy Phys. 01 (2010) 026; A. Gorsky, P. N. Kopnin, and A. V. Zayakin, Phys. Rev. D **83**, 014023 (2011); V. A. Rubakov, arXiv:1005.1888; A. Gynther, K. Landsteiner, F. Pena-Benitez, and A. Rebhan, J. High Energy Phys. 02 (2011) 110; V. D. Orlovsky and V. I. Shevchenko, Phys. Rev. D **82**, 094032 (2010); L. Brits and J. Charbonneau, Phys. Rev. D **83**, 126013 (2011); A. V. Sadofyev and M. V. Isachenkov, Phys. Lett. B **697**, 404 (2011); D. Hou, H. Liu, and H.-c. Ren, J. High Energy Phys. 05 (2011) 046; C. Hoyos, T. Nishioka, and A. O'Bannon, J. High Energy Phys. 10 (2011) 084; A. Yamamoto, Phys. Rev. D **84**, 114504 (2011); V. P. Nair, R. Ray, and S. Roy, Phys. Rev. D **86**, 025012 (2012); D. T. Son and N. Yamamoto, arXiv:1203.2697.
[6] K. Fukushima, D. E. Kharzeev, and H. J. Warringa, Nucl. Phys. **A836**, 311 (2010).
[7] P. V. Buividovich, M. N. Chernodub, E. V. Luschevskaya, and M. I. Polikarpov, Phys. Rev. D **80**, 054503 (2009); M. Abramczyk, T. Blum, G. Petropoulos, and R. Zhou, Proc. Sci., LAT2009 (**2009**) 181.
[8] S. i. Nam, Phys. Rev. D **80**, 114025 (2009); **82**, 045017 (2010).
[9] G. Basar, G. V. Dunne, and D. E. Kharzeev, Phys. Rev. D **85**, 045026 (2012).
[10] K. Fukushima, D. E. Kharzeev, and H. J. Warringa, Phys. Rev. Lett. **104**, 212001 (2010).
[11] H. Gies, Eur. Phys. J. D **55**, 311 (2009); M. Marklund and J. Lundin, Eur. Phys. J. D **55**, 319 (2009); G. V. Dunne, Eur. Phys. J. D **55**, 327 (2009).
[12] D. Kharzeev, A. Krasnitz, and R. Venugopalan, Phys. Lett. B **545**, 298 (2002); T. Lappi and L. McLerran, Nucl. Phys. **A772**, 200 (2006);
[13] H. Minakata and B. Muller, Phys. Lett. B **377**, 135 (1996); V. Skokov, A. Y. Illarionov, and V. Toneev, Int. J. Mod. Phys. A **24**, 5925 (2009); K. Tuchin, Phys. Rev. C **82**, 034904 (2010); V. Voronyuk, V. D. Toneev, W. Cassing, E. L. Bratkovskaya, V. P. Konchakovski, and S. A. Voloshin, Phys. Rev. C **83**, 054911 (2011); W.-T. Deng and X.-G. Huang, Phys. Rev. C **85**, 044907 (2012).
[14] G. D. Moore and M. Tassler, J. High Energy Phys. 02 (2011) 105.
[15] D. Kharzeev, Phys. Lett. B **633**, 260 (2006); D. Kharzeev and A. Zhitnitsky, Nucl. Phys. **A797**, 67 (2007).
[16] S. A. Voloshin, Phys. Rev. C **70**, 057901 (2004).
[17] B. I. Abelev *et al.* (STAR Collaboration), Phys. Rev. Lett. **103**, 251601 (2009); Phys. Rev. C **81**, 054908 (2010).
[18] P. Christakoglou, J. Phys. G **38**, 124165 (2011).
[19] A. Bzdak, V. Koch, and J. Liao, Phys. Rev. C **81**, 031901 (2010); M. Asakawa, A. Majumder, and B. Muller, Phys. Rev. C **81**, 064912 (2010); J. Liao, V. Koch, and A. Bzdak, Phys. Rev. C **82**, 054902 (2010); H. Petersen, T. Renk, and S. A. Bass, Phys. Rev. C **83**, 014916 (2011); A. Bzdak, V. Koch, and J. Liao, Phys. Rev. C **83**, 014905 (2011); B. Muller and A. Schafer, Phys. Rev. C **82**, 057902 (2010).
[20] V. I. Ritus, Ann. Phys. (Berlin) **69**, 555 (1972); V. I. Ritus, Zh. Eksp. Teor. Fiz. **75**, 1560 (1978); [Sov. Phys. JETP **48**, 788 (1978)].
[21] M. E. Peskin and D. V. Schroeder, *An Introduction to Quantum Field Theory* (Perseus Books, Reading, MA, 1995).
[22] A. I. Nikishov, Zh. Eksp. Teor. Fiz. **57**, 1210 (1969).
[23] N. B. Narozhnyi and A. I. Nikishov, Yad. Fiz. **11**, 1072 (1970); Sov. J. Nucl. Phys. **11**, 596 (1970)].
[24] J. Ambjorn, J. Greensite, and C. Peterson, Nucl. Phys. **B221**, 381 (1983).

[25] Y. Kluger, J. M. Eisenberg, B. Svetitsky, F. Cooper, and E. Mottola, Phys. Rev. D **45**, 4659 (1992).
[26] S. P. Gavrilov and D. M. Gitman, Phys. Rev. D **78**, 045017 (2008).
[27] N. Tanji, Ann. Phys. (Berlin) **324**, 1691 (2009).
[28] F. V. Bunkin and I. I. Tugov, Sov. Phys. Dokl. **14**, 678 (1970).
[29] G. V. Dunne, arXiv:hep-th/0406216.
[30] S. P. Kim and D. N. Page, Phys. Rev. D **73**, 065020 (2006).
[31] T. D. Cohen and D. A. McGady, Phys. Rev. D **78**, 036008 (2008).
[32] W. Heisenberg and H. Euler, Z. Phys. **98**, 714 (1936).
[33] L. F. Urrutia, Phys. Rev. D **17**, 1977 (1978); V. P. Barashev, A. E. Shabad, and S. M. Shvartsman, Yad. Fiz. **43**, 964 (1986); [Sov. J. Nucl. Phys. **43**, 617 (1986)]; C. Schubert, Nucl. Phys. **B585**, 407 (2000).
[34] S. L. Adler, Ann. Phys. (Berlin) **67**, 599 (1971); W.-y. Tsai, Phys. Rev. D **10**, 2699 (1974); A. E. Shabad, Ann. Phys. (Berlin) **90**, 166 (1975).
[35] K. Fukushima, Phys. Rev. D **83**, 111501 (2011); E. J. Ferrer, V. de la Incera, and A. Sanchez, Phys. Rev. Lett. **107**, 041602 (2011); H. Gies and L. Roessler, Phys. Rev. D **84**, 065035 (2011); F. Karbstein, L. Roessler, B. Dobrich, and H. Gies, Int. J. Mod. Phys. Conf. Ser. **14**, 403 (2012); N. Sadooghi and F. Taghinavaz, Phys. Rev. D **85**, 125035 (2012).